Progress In Electromagnetics Research Letters, Vol. 103, 39–48, 2022

A New Structure for the Coaxial Magnetic Gear with HTS Bulks for Fitness Car

Yan Wang[1] and Libing Jing[2, *]

Abstract—This paper proposes a novel coaxial magnetic gear (CMG) with eccentric permanent magnet structure and unequal Halbach arrays for achieving sinusoidal air-gap flux density and high output torque. The proposed model has a high temperature superconducting (HTS) bulks to replace the epoxy resin in the conventional stationary ring. According to the Meissner effect and one-sided field, the HTS bulks could enhance the modulation effect. The permanent magnets (PMs) on the inner and outer rotors are distributed in Halbach array, in which the PMs are arranged regularly on the outer rotor, and the inner rotor is an eccentric structure. So the inner nonuniform air gap can be obtained. The proposed model with the pole pairs of 4 and 17 for the inner and outer rotors is established, and using finite element analysis (FEA) a calculated torque is up to $350.8\,\mathrm{N}\cdot\mathrm{m}$. It is 2.16 times of the torque of conventional CMG.

1. INTRODUCTION

Magnetic gear, as a kind of non-contact transmission component, has many advantages, such as no friction, oil-pollution free, low maintenance, and easy installation [1]. The concept of magnetic gear was first put forward in 1913, but the torque density of conventional magnetic gear is low and cannot meet the needs of industrial production. In 2001, the coaxial magnetic gear (CMG) was proposed by Atallah and Howe [2]. As shown in Fig. 1, the utilization rate of permanent magnet is very high, because each permanent magnet on two rotors is involved in the torque transmission. Magnetic gear has many applications in the field of low speed and high torque transmission, such as wind power generation [3], electric vehicles [4], and tidal power generation [5]. At the same time, the CMG can also be used in the fitness car. The fitness person drives the high-speed inner rotor by stepping on the outer rotor with low speed and high torque, so as to achieve the effect of exercise.

Torque density and torque ripple are usually used for measuring the transmission capacity and stability of CMG. In [6], a 3-D CMG with Halbach arrays is established. The results show that the model can reduce the harmonic component of flux and improve the output torque. Authors in [7] proposed a flux focusing CMG, and due to the effect of tangential polarized magnetic field concentration, this kind of CMG has high torque density.

CMG with high temperature superconducting (HTS) bulks were also recently presented in [8, 9], which have high torque density. The linear MG with HTS bulks is presented in [10], and magnetic flux density and thrust force transmission capacity are higher than the conventional MG. In [11], a CMG topology using superconductors instead of PMs is proposed, which can produce a large torque density. A novel single PM array stationary CMG with flux modulation teeth made of HTS material is proposed in [12]. The maximum output torque of the CMG is 1.73 times that of the ferromagnetic

Received 9 January 2021, Accepted 11 February 2022, Scheduled 21 February 2022

* Corresponding author: Libing Jing (jinglibing163@163.com).

[1] College of Physical Education, China Three Gorges University, Yichang 443002, China. [2] College of Electrical Engineering & New Energy, China Three Gorges University, Yichang 443002, China.

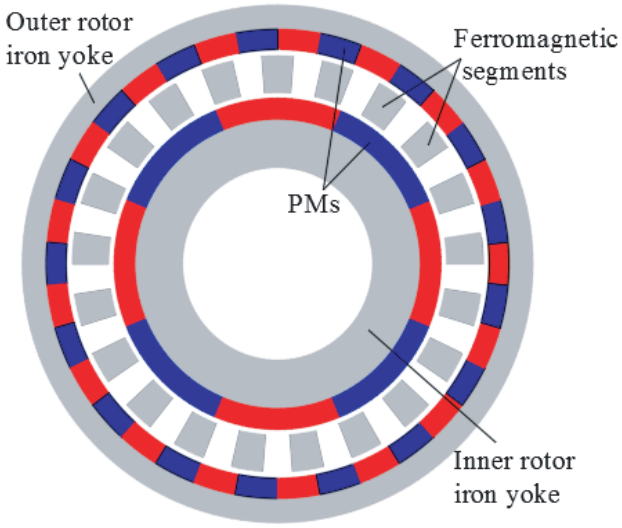

Figure 1. Overview of the conventional magnetic gear.

toothed gear. At present, these designs have high torque density, but there are many defects, such as complex structure, large torque ripple, and high technical processing requirements.

In this paper, a CMG with an eccentric permanent magnet structure and unequal Halbach arrays is proposed to get sinusoidal air-gap flux density and high output torque. In this model, HTS bulks are also used for replacing the epoxy resin in the stationary ring, and the purpose is to improve the modulation effect. In Section 2, the topology of HTS bulks CMG is introduced in detail. In Section 3, the proposed general pattern is applied to the magnetic gear; the characteristics of proposed model are calculated by FEA and compared with those of conventional CMG. Finally, some conclusions are drawn in Section 4.

2. HTS BULKS CMG

Figure 2 shows the structure of the proposed HTS bulks CMG. Similar to the conventional CMG, it is also composed of two rotors and a stationary ring. PMs are installed on the surface of the two rotors, and HTS replaces the epoxy resin in the stationary ring. The stationary ring is fixed between the inner and outer PM rotors to modulate the air gap magnetic field. The distribution of permanent magnets

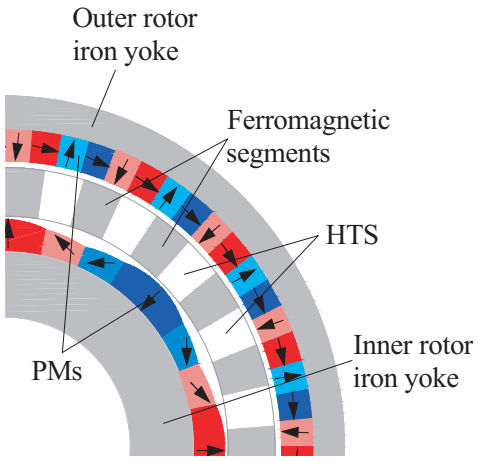

Figure 2. Overview of the proposed CMG.

on the outer rotor is a regular Halbach array, and each pole is divided into two small pieces of PMs, which are composed of radial and tangential polarized PMs alternately. The distribution of the PM on the inner rotor is an eccentric structure, and each pole is divided into three small PMs, in which the magnetization is sinusoidal.

The structure of PMs with eccentric and unequal Halbach arrays on the inner rotor is shown in Fig. 3. The shape of the eccentric pole can be used to change the air gap. The nonuniform air gap makes the magnetic field waveform close to the sinusoidal distribution, so as to improve the magnetic density harmonic.

It can be seen from Fig. 3 that there are 3 small pieces of PMs on each pole. PM is an eccentric structure with different lengths and widths. O_1 and R_1 are the centre and radius of the arc AB and arc DE, respectively, and their eccentricity is OO_1. O_2 and R_2 are the centre and radius of the arc BCD, respectively, and its eccentricity is OO_2. The middle PM is magnetized radially, and the magnetization angles of the small PMs on both sides are α and $-\alpha$, respectively.

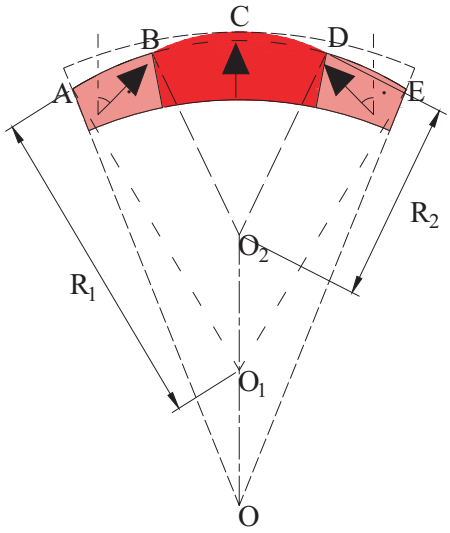

Figure 3. Eccentric PM structure.

In order to enhance the modulation effect of magnetic field, HTS bulks is used to replace epoxy resin in the stationary ring. Based on the Meissner effect, it can be seen that the HTS bulks can effectively inhibit the magnetic field penetration under the critical temperature. Fig. 4 shows the sectional view of the HTS bulks, which consists of 4 parts, namely, superconducting material, condensate, vacuum chamber, and carbon fibers frame. The HTS bulks used in the proposed magnetic gear are made from yttrium barium copper oxide (YBCO) materials. When the temperature is lower than 77 K,

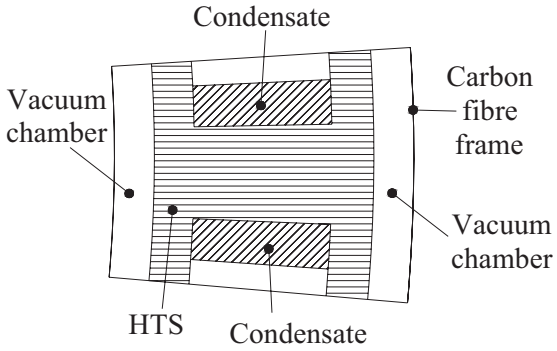

Figure 4. HTS bulk.

the superconducting material begins to exert magnetic resistance characteristics, which ensures that the magnetic flux will not pass through the magnetic resistance bulks and make it pass through the ferromagnetic segment as much as possible. The carbon fiber frame can reduce the mass of the stationary ring. The condensates can ensure that the superconducting materials work in the appropriate temperature range. The circulating cooling of condensate in the pipeline can be completed by the external HTS motor, and the vacuum chamber can play the role of insulation, which will help to reduce the thermal leakage.

Each pole of the outer rotor has two small PMs, which are distributed in a standard Halbach array. The expression of magnetization direction of each PM is as follows:

$$\vec{M} = M_r \vec{r} + M_\theta \vec{\theta} \tag{1}$$

where M_r and M_θ are

$$M_r = \sum_{n=1,3,5\ldots}^{\infty} M_{rn}(n) \cos[np(\theta - \theta_0)] \tag{2}$$

$$M_\theta = \sum_{n=1,3,5\ldots}^{\infty} M_{\theta n}(n) \sin[np(\theta - \theta_0)] \tag{3}$$

where p is the number of pole pairs, and θ_0 is the offset angle between the permanent magnet and the initial reference position. M_{rn} and $M_{\theta n}$ are

$$M_{rn}(n) = \frac{4B_r}{\mu_0 \pi} \frac{1}{n} \sin\left(\frac{n\pi}{4}\right) \cdot \left\{1 + \sum_{k=2}^{m} \cos\left[\frac{(k-1)\pi}{2}\right] \cos\left[\frac{(k-1)n\pi}{2}\right]\right\} \tag{4}$$

$$M_{\theta n}(n) = \frac{4B_r}{\mu_0 \pi} \frac{1}{n} \sin\left(\frac{n\pi}{4}\right) \cdot \left\{\sum_{k=2}^{m} \sin\left[\frac{(k-1)\pi}{2}\right] \sin\left[\frac{(k-1)n\pi}{2}\right]\right\} \tag{5}$$

where K is the kth PM segment of each pole, μ_0 the permeability of vacuum, and B_r the remanence of the PM.

Based on the theory of magnetic field modulation, a large number of harmonics exist in the inner and outer air gap magnetic fields. The pole-pair number of the harmonics in the air gap can be expressed as follows,

$$P_{ijk} = kN_s + jP_{in}, \quad j = 1, -1, \quad k = 1, 2, \ldots, \infty \tag{6}$$

$$P_{ojk} = kN_s + jP_{out}, \quad j = 1, -1, \quad k = 1, 2, \ldots, \infty \tag{7}$$

where N_s=P_{in} + P_{out}, which is the number of ferromagnetic segments, and P_{in} and P_{out} are the pole pairs of the two rotors, respectively.

The corresponding speeds of the inner and outer rotors are ω_1 and ω_2, respectively. Their relations are as follows:

$$G_r = -\frac{\omega_2}{\omega_1} = -\frac{P_{in}}{P_{out}} \tag{8}$$

where G_r is the gear ratio, and the "$-$" indicates that the rotation directions of two rotors are opposite.

3. PERFORMANCES ANALYSIS

The design parameters of the HTS bulks CMG are given in Table 1. In this model, $P_{in} = 4$ and $P_{out} = 17$, respectively. Axial length of proposed CMG is 40 mm. Each pole of the inner and outer rotor PMs is divided into 3 pieces and 2 pieces, respectively.

3.1. Flux Density and Harmonics

Figure 5 shows the magnetic flux lines calculated by FEA for two kinds of CMG.

Table 1. Main parameters of the HTS bulks CMG.

Quantity	Value
Inner radius of the inner rotor yoke	40 mm
Outer radius of inner rotor yoke	60 mm
R_1	48.74 mm
R_2	30 mm
Minimum length of inner air gap	1 mm
Thickness of stationary ring	15 mm
The length of outer air gap	1 mm
Length of PMs on the outer rotor	10 mm
Inner radius of the outer rotor yoke	87 mm
Remanence of PM	1.1 T
α	45°
OO_1	20 mm
OO_2	40 mm

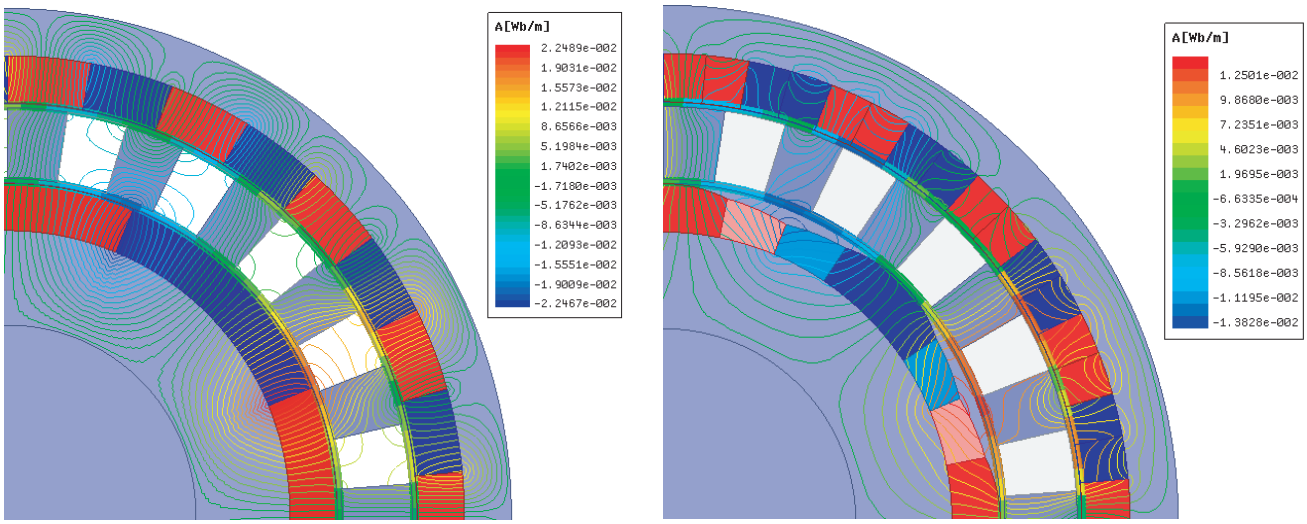

(a) (b)

Figure 5. Magnetic flux line distributions. (a) Conventional. (b) Proposed.

As can be seen from Fig. 5, the magnetic flux lines in the yoke of the inner and outer rotors of the proposed HTS bulks CMG are much fewer than that of the conventional CMG. The yoke of the two rotors can be reduced, and the weight and volume can also be reduced. The magnetic flux lines do not pass through HTS bulks, thus reducing the magnetic flux leakage.

Figure 6 shows the comparison of the inner air gap magnetic flux density of the two CMGs. From the simulation results, it can be seen that the air gap magnetic flux density of the proposed model has better sinusoidal characteristics.

The harmonic spectrum of the inner air gap flux density is shown in Fig. 7. It can be seen that the flux density amplitudes of some harmonics are greatly reduced. Based on the principle of magnetic field modulation and Meissner effect, the numbers of harmonics that contribute greatly to torque transmission in the inner air gap are 4, 17, 25, 38, and 46, which are all effective harmonics. However, by comparison, the proposed HTS bulks CMG has an obvious inhibitory effect on the harmonic components of the 12th,

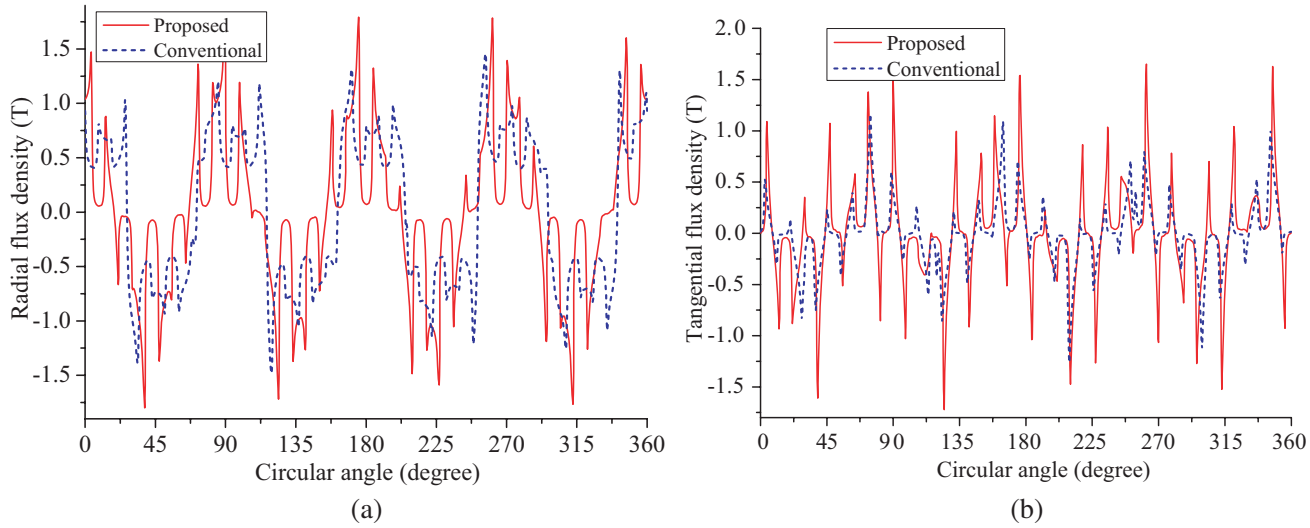

Figure 6. Flux density in the inner air gap: (a) Radial component, (b) Tangential component.

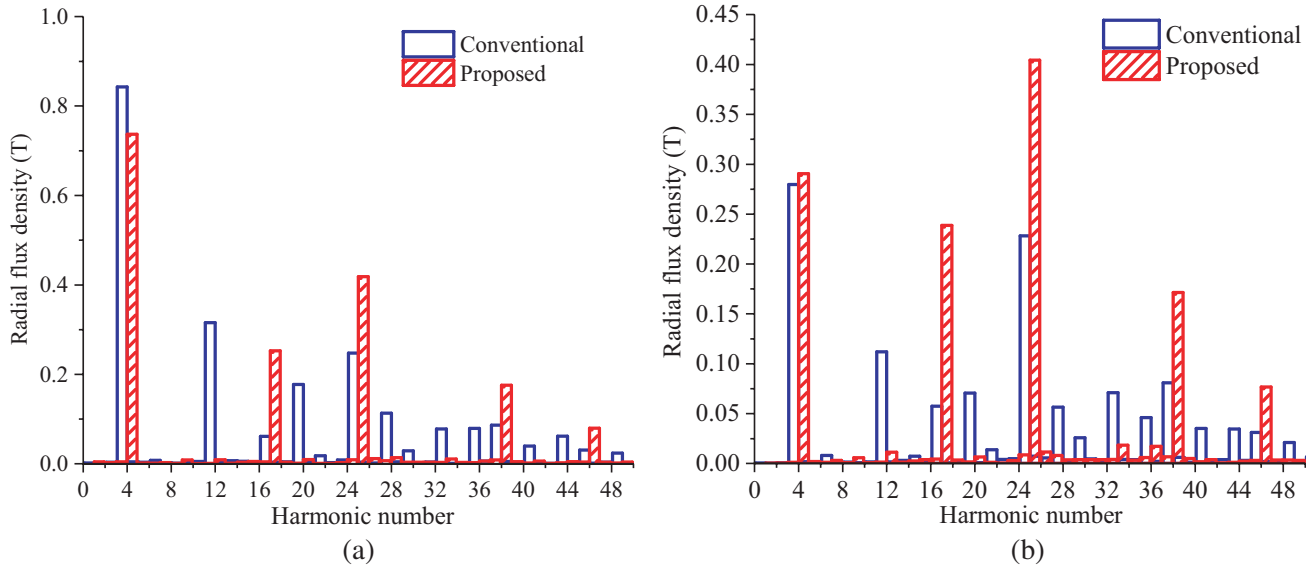

Figure 7. Harmonic spectrum in the inner air gap: (a) Radial, (b) Tangential.

20th, 28th, 33rd, 36th, and 41st order. The suppression of these harmonics is helpful to reduce the torque ripple of the inner rotor.

Figure 8 shows the comparison of the outer air gap magnetic flux densities of the two CMGs.

The harmonic spectrum of the external air gap flux density is shown in Fig. 9. The results show that the main harmonic amplitudes of the proposed model are larger than that of the conventional CMG, which is beneficial for improving the output torque. Especially, the amplitudes of 17th, 25th, and 38th harmonics are very large. In addition, the 12th, 20th, 28th, and 33rd harmonic components of the proposed HTS bulks CMG are very small, which has no effect on the torque ripple of the CMG.

3.2. Torque

The static torque curve of the proposed HTS bulks CMG is shown in Fig. 10. The specific method is to fix the outer rotor and the stationary ring. The rotating speed of the inner rotor is 85 r/min. The results show that the phase difference of the torque curve of the inner and outer rotors is 180°, and the

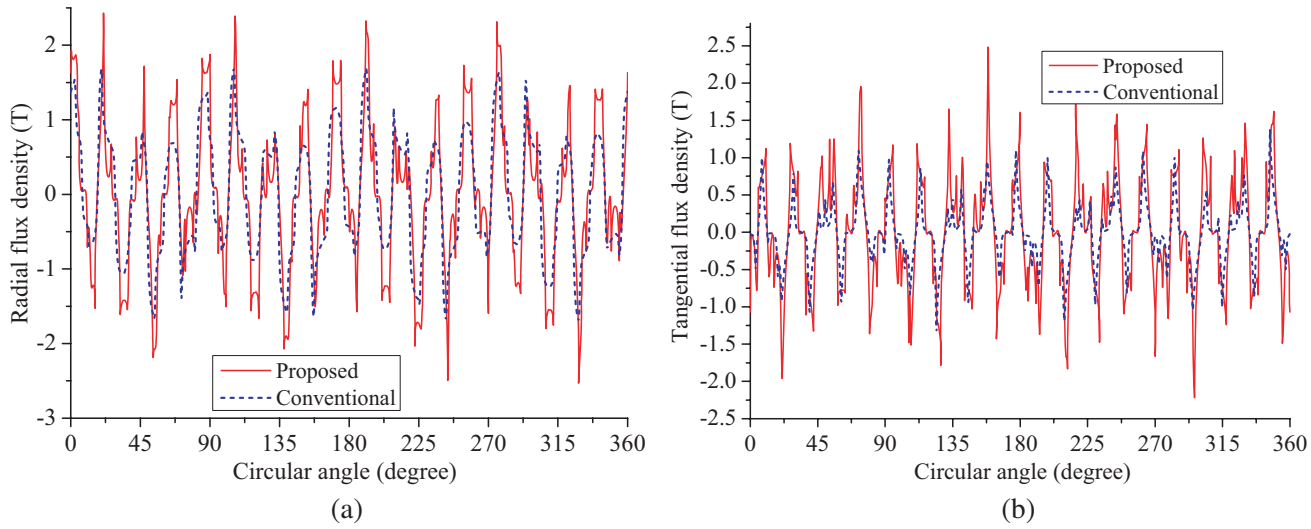

Figure 8. Flux density in the outer air gap: (a) Radial component, (b) Tangential component.

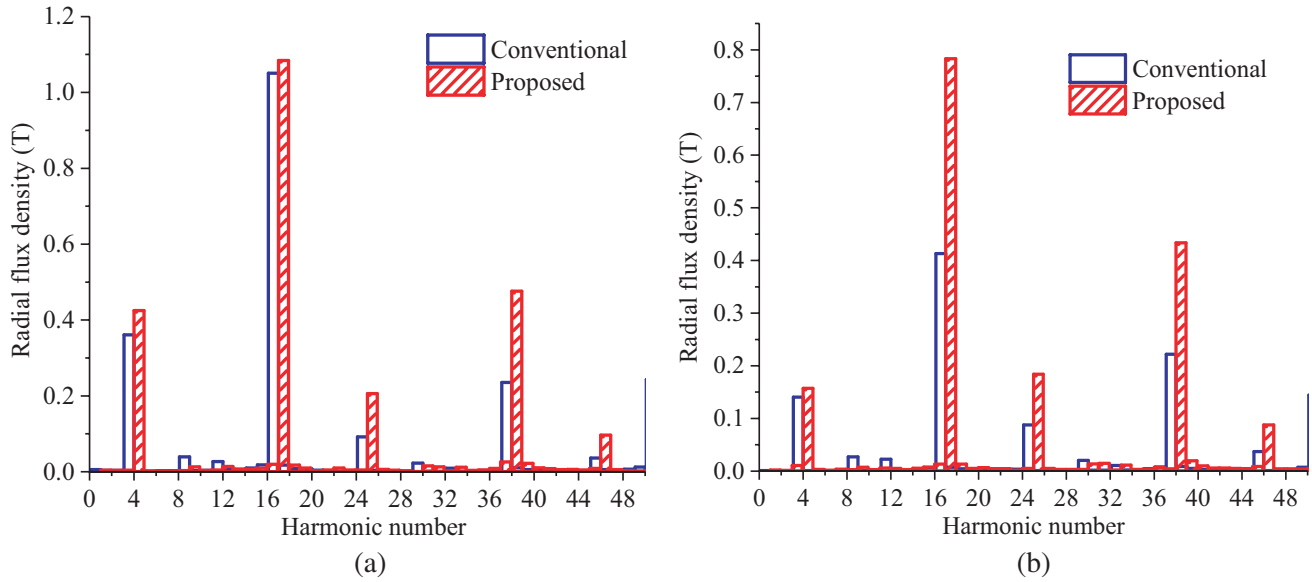

Figure 9. Harmonic spectrum in the outer air gap: (a) Radial, (b) Tangential.

torque curve is sinusoidal with the angle change.

Figure 11 shows the comparison of the electromagnetic torque of the two CMGs. The specific method is to fix the stationary ring, and the inner and outer rotors rotate at the speeds of 20 r/min and 85 r/min in opposite directions, respectively. The comparison shows that the transmission ratio is equal to the gear ratio, but the inner and outer rotor torques of the proposed model reach 82.53 N · m and 350.8 N · m, respectively, which is 2.16 times that of the conventional model. At the same time, the torque ripple of the proposed model is much smaller than that of the conventional model.

Iron loss is an important part of magnetic gear transmission loss. Fig. 12 shows the no-load iron loss of the CMG at different speeds. When the rotating speed of inner rotor is below 400 r/min, the two losses are basically the same. When the rotating speed of inner rotor is 1100 r/min, the iron loss of the proposed HTS bulks CMG is 189.3 W, while that of the conventional CMG is 354 W. It is also proved that the novel proposed CMG can reduce the iron loss by 46.5%.

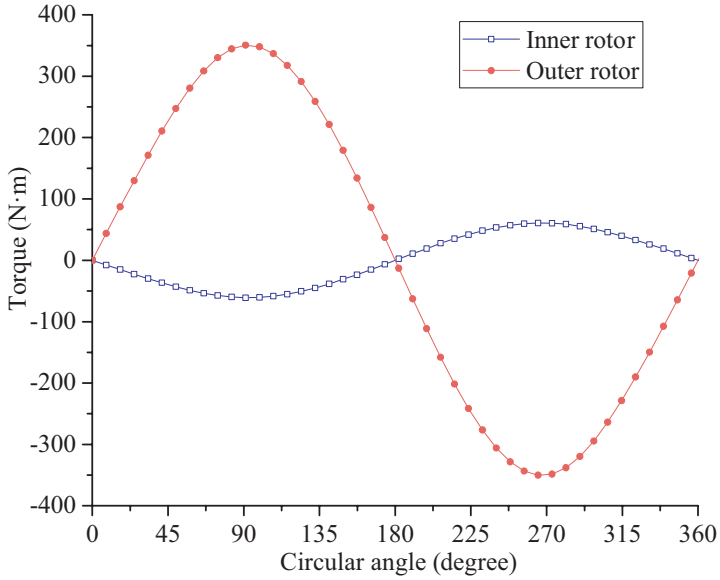

Figure 10. Torque transmission capacity.

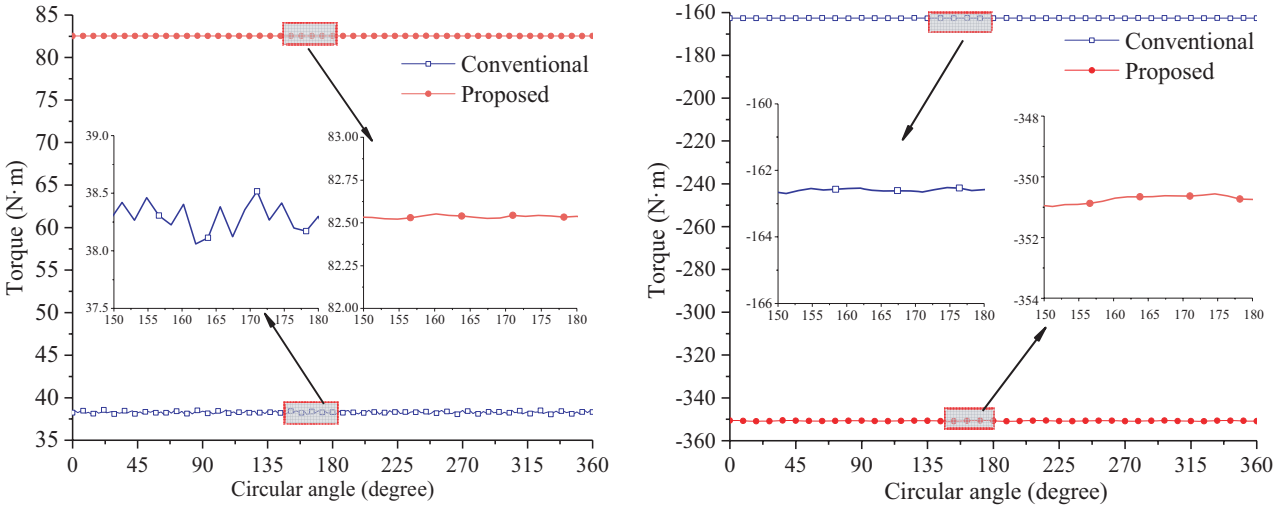

Figure 11. Electromagnetic torque. (a) Inner rotor, (b) Outer rotor.

Table 2. Performance comparison of CMG.

Quantity	Conventional	Proposed
Torque of the inner rotor (N · m)	38.2	82.53
Torque of the Outer rotor (N · m)	162.4	350.8
Iron loss (W)	354	189.3

Table 2 lists the performance comparison between the conventional CMG and the proposed CMG.

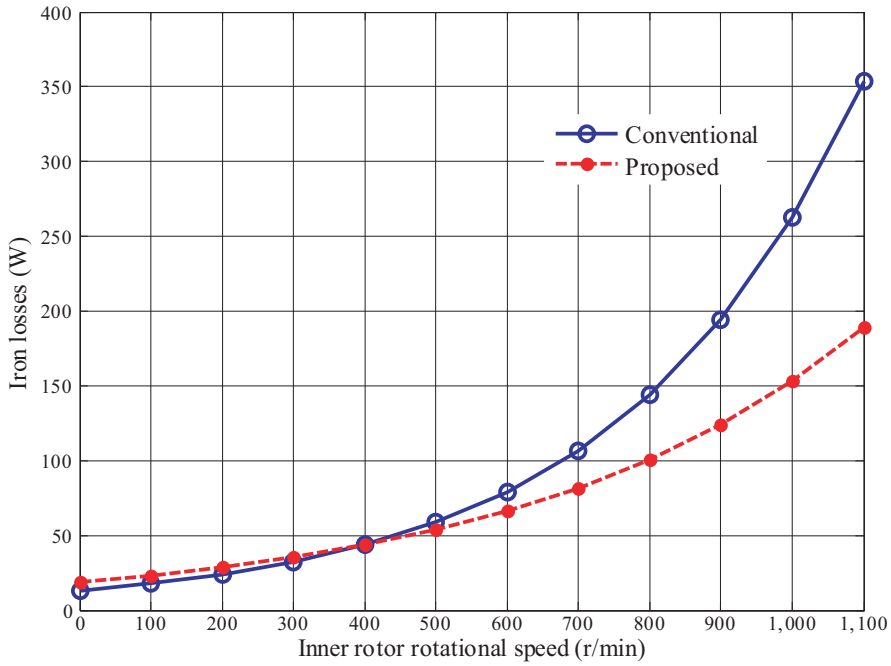

Figure 12. Iron losses at different rotational speeds.

4. CONCLUSION

A novel HTS bulks CMG with nonuniform air gap and unequal Halbach arrays has been presented and analyzed in this paper. There are two advantages of HTS bulks instead of epoxy resin. One is to improve the effect of magnetic field modulation, and the other is to suppress magnetic flux leakage. On the inner rotor, the nonuniform air gap can be obtained by an eccentric PM structure, which helps to obtain sinusoidal flux density and reduce torque ripple. Halbach array on the outer rotor can increase the magnetic flux density and reduce the amplitude of non-working harmonic. The torque of the proposed CMG is 2.16 times of that of the conventional CMG, and the iron loss is 46.5% less than that of the conventional CMG.

ACKNOWLEDGMENT

This work was supported by the National Natural Science Foundation of China (Project No.: 51707072), China Postdoctoral Science Foundation (Project No.: 2018M632855).

REFERENCES

1. Jing, L., Z. Huang, J. Chen, and R. Qu, "An asymmetric pole coaxial magnetic gear with unequal Halbach arrays and spoke structure," *IEEE Trans. Appl. Supercond.*, Vol. 30, No. 4, 1–4, Jun. 2020.
2. Atallah, K. and D. Howe, "A novel high-performance magnetic gear," *IEEE Trans. Magn.*, Vol. 37, No. 4, 2844–2846, Jul. 2001.
3. Padmanathan, P. and J. Z. Bird, "A continuously variable magnetic gear," *IEEE Proc. IEMDC*, 367–373, May 2013.
4. Fan, Y., L. Gu, Y. Luo, X. Han, and M. Cheng, "Investigation of a new flux-modulated permanent magnet brushless motor for EVs," *The Scientific World Journal*, Vol. 2014, Art. No. 540797, Apr. 2014.

5. Du, Y., K. T. Chau, and M. Cheng, "A linear stator permanent magnet vernier HTS machine for wave energy conversion," *IEEE Trans. Appl. Supercond.*, Vol. 22, No. 3, Art. No. 5202505, Jun. 2012.
6. Frank, N. W., S. Pakdelian, and H. A. Toliyat, "Passive suppression of transient oscillations in the concentric planetary magnetic gear," *IEEE Trans. Energy Convers.*, Vol. 26, No. 3, 933–939, Sep. 2011.
7. Uppalapati, K. K., J. Z. Bird, and J. Wright, "A magnetic gearbox with an active region torque density of 239 Nm/L," *IEEE Energy Conversion Congress and Exposition*, 1423–1428, 2014.
8. Jian, L., K. Chau, W. Li, and J. Li, "A novel coaxial magnetic gear using bulk HTS for industrial applications," *IEEE Trans. Appl. Supercond.*, Vol. 20, No. 3, 981–984, Jun. 2010.
9. Cansiz, A. and E. Akyerden, "The use of high temperature superconductor bulk in a co-axial magnetic gear," *Cryogenics*, Vol. 98, 80–86, 2019.
10. Liu, C., H. Zhu, and R. Dong, "Linear magnetic gear with HTS bulks for wave energy conversion," *IET Renew. Power Gen.*, Vol. 13, No. 13, 2430–2434, 2019.
11. Campbell, A., "A superconducting magnetic gear," *Supercond. Sci. Technol.*, Vol. 29, No. 5, 054008, 2016.
12. Yin, X., Y. Fang, and P. Pfister, "A novel single-PM-array magnetic gear with HTS bulks," *IEEE Trans. Appl. Supercond.*, Vol. 27, No. 4, ID. 5202705, Jun. 2017.